Electron kinetic effects in atmosphere breakdown by an intense electromagnetic pulse

A. A. Solovyev and V. A. Terekhin
Russian Federal Nuclear Center, All-Russian Scientific Research Institute of Experimental Physics, Sarov 607190, Russia

V. T. Tikhonchuk
P. N. Lebedev Physics Institute, Russian Academy of Science, Moscow 117924, Russia

L. L. Altgilbers
Missile Defense and Space Technology Center, Huntsville, Alabama
(Received 28 April 1999)

A physical model is proposed for description of electron kinetics driven by a powerful electromagnetic pulse in the Earth's atmosphere. The model is based on a numerical solution to the Boltzmann kinetic equation for two groups of electrons. Slow electrons (with energies below a few keV) are described in a two-term approximation assuming a weak anisotropy of the electron distribution function. Fast electrons (with energies above a few keV) are described by a modified macroparticle method, taking into account the electron acceleration in the electric field, energy losses in the continuous deceleration approximation, and the multiple pitch angle scattering. The model is applied to a problem of the electric discharge in a nitrogen, which is preionized by an external gamma-ray source. It is shown that the runaway electrons have an important effect on the energy distribution of free electrons, and on the avalanche ionization rate. This mechanism might explain the observation of multiple lightning discharges observed in the Ivy-Mike thermonuclear test in the early 1950's.
[S1063-651X(99)16610-8]

PACS number(s): 52.20.−j, 51.50.+v, 52.65.−y, 52.80.−s

I. INTRODUCTION

The interaction of powerful electromagnetic pulses (EMP) with the atmosphere and ionosphere is an important part of many practical applications, such as long-range communications, artificial ionosphere modification, and remote monitoring of unsanctioned nuclear explosions. Numerous nonlinear effects, which have not been fully investigated, are associated with the propagation of intense EMP. Two important nonlinear effects are the ionization of air and the production of a plasma in the tail of the electromagnetic pulse, which results in the reduction of pulse energy and a change in the pulse shape. The air breakdown threshold, which is known for normal conditions, may change significantly in a natural environment. In particular, even small amounts of fast electrons, with energies well above the ionization energy of air, might dramatically reduce its breakdown threshold. Because of the low collision rates of these fast electrons, they can initiate avalanche ionization. This ''runaway'' mechanism for air breakdown was recently proposed [1] to explain high altitude lightning discharges, where the cosmic rays were considered as a source of fast electrons. Numerical solutions of the electron kinetic equation [2] demonstrated that a significant decrease in the air breakdown threshold under conditions in which a small number of relativistic electrons was present in the air. The sharp increase in the ionization rate due to the presence of runaway electrons have an energy in the range of the ionization potential for air has also been demonstrated [3] by an approximate analytical solution of the electron kinetic equation. However, a more detailed description of electron inelastic collisions is required in order to obtain the electron distribution in the real atmosphere and to investigate secondary processes, such as plasma chemical reactions and optical emissions of excited molecules.

Standard approaches to the numerical solving the Boltzmann kinetic equation are usually very inefficient due to the broad range of electron energies (from fractions of an eV to tens of MeV) that must be accounted for. However, a weak coupling between two groups of electrons, fast and slow electrons, offers an effective method for optimizing the numerical solution of the electron kinetic equation. In this paper, a model is presented for describing the kinetics of electrons driven by powerful EMP in the Earth's atmosphere. It combines macroparticle and finite difference methods by using a finite difference algorithm to solve the Boltzmann kinetic equation for the low energy electrons (less than a few keV) and a macroparticle description to describe fast, high energy electrons. The collisions of fast electrons are accounted for in the approximation of continuous deceleration and multiple pitch angle scattering. This hybrid description of electrons is an important addition to current models in that it accurately describes the electron distribution function over the energy range from a few eV up to relativistic energies. At the same time, this approach ensures good performance is maintained for its various applications.

This model has been benchmarked for the case of nitrogen gas avalanche ionization by a dc electric field. By comparing the experimental data on the electron mobility and the avalanche rates with the calculated values, the accuracy and performance of the code could be checked. The model has also been applied to the avalanche ionization of the nitrogen, which is preionized by externally applied gamma rays. It was found that a relatively small initial number of fast electrons can reduce the breakdown threshold by an order of magnitude. It has been suggested that this effect could be an explanation for the multiple lightning discharges observed dur-

ing the Ivy-Mike thermonuclear test in the early 1950's [4], a phenomenon which has not been explained to date [5].

The second section of the paper is devoted to a description of the basic equations of the models for both the slow and fast electrons and how the two groups exchange particles and energy. The numerical algorithms are also briefly discussed in this section along with a comparison of the calculated and measured electron mobility of molecular nitrogen in a dc electric field. The third section is devoted to an analysis of the electron kinetics in nitrogen gas in an external dc electric field, where the discharge is seeded by relativistic electrons. The high energy seed electrons dramatically change the discharge characteristics. It significantly decreases the breakdown threshold and changes the relationship between the populations of fast and slow electrons. The runaway effect is also applied for analysis of the Ivy-Mike test. Finally, the fourth section contains a summary and concluding remarks.

II. FORMULATION OF THE MODEL

The problem of the interaction of powerful EMP with the atmosphere can be divided into two parts. The first is an analysis of electron dynamics in electric and magnetic fields, taking into account their collisions with neutral molecules and possible runaway electrons that may achieve relativistic velocities. The solution of the kinetic equation for the electron distribution function, $f(t,\mathbf{r},\mathbf{p})$, defines the current, $\mathbf{j}=-e\int d\mathbf{p}\mathbf{v}f$, that is needed for the second part of the problem, which is the self-consistent description of the spatial and temporal evolution of the pulse electric, $\mathbf{E}$, and magnetic, $\mathbf{B}$, fields behind the ionization front according to Maxwell's equations:

$$\frac{\partial}{\partial t}\mathbf{B}=-c\nabla\times\mathbf{E},\quad \frac{\partial}{\partial t}\mathbf{E}+4\pi\mathbf{j}=c\nabla\times\mathbf{B}. \tag{1}$$

This paper is devoted predominantly to an analysis of the former problem of electron kinetics. Since attention is to be focused on altitudes from the ground to 150–200 km in the atmosphere, where the characteristic electron mean free path (from a few meters up to 100 m) is comparable to the gyroradius of electrons, but much smaller than the wavelength of the EMP and the scale length of variations of the density and temperature of the atmosphere, the convective term is neglected. The problem is thus reduced to solving the homogeneous kinetic equations [6]:

$$\frac{\partial f}{\partial t}-e\left[\mathbf{E}+\frac{\mathbf{v}}{c}\times(\mathbf{B}+\mathbf{B}_0)\right]\frac{\partial f}{\partial\mathbf{p}}=NJ^{st}, \tag{2}$$

where $\mathbf{B}_0$ is the geomagnetic field, $\mathbf{v}=\mathbf{p}/m\gamma$ and $\mathbf{p}$ are the electron velocity and momentum, respectively, $\gamma=\sqrt{1+p^2/m^2c^2}$ is the relativistic factor, $-e$ and m are the electron charge and mass, N is the density of neutral particles, and J^{st} is the Boltzmann electron-neutral collision integral. The spatial dependence of the electron distribution function is accounted for indirectly through its dependence on electric and magnetic fields.

Different methods have been proposed for solving Eq. (2), each of which has its own attributes. The electron collision integral is a most complicated part the problem, since each electron collision dramatically changes the particle trajectory and, eventually redistributes the particles in phase space. A specific feature of the model presented in this paper is that it takes into account the effects of gamma-ray produced Compton electrons on the gas ionization dynamics, and, therefore, requires that a very broad energy range (from less than 1 eV up to MeV energies) be considered. All of the known algorithms are ineffective in dealing with this broad energy range. In order to overcome this limitation of current models, it was decided to divide the entire electron population into two groups: slow electrons with energies ranging from the ionization potential of the chemical species in the atmosphere up to a few keV, and fast electrons with energies from a few keV up to relativistic energies. This is accomplished by applying two different methods to solve the kinetic equation; that is, one method is used to solve the equation for the slow electrons and another method for the fast electrons. At the same time, the exchange of energy and particles between the two groups was taken into account. Assuming that the low energy electrons, $\epsilon<\epsilon_g$, where ϵ is kinetic energy, are treated as a continuous medium and that the slow electron distribution function is weakly anisotropic, the kinetic equation, Eq. (2), can be solved by using a finite difference algorithm [7]. Assuming that the fast electrons are discrete particles, their interaction with neutral particles can be approximated as a continuous deceleration and their multiple pitch angle scattering can be taken into account [8,9].

A. Slow electron kinetics

Under atmospheric conditions, collisions play an important role in the dynamics of slow electrons ($\epsilon<\epsilon_g$ $\sim$ a few keV). Therefore, their distribution function can be considered to be weakly anisotropic and can be approximated by using two terms. Since this approximation is well known [6], only the main elements of the slow electron model are discussed, so that more attention can be focused on modeling the fast electrons and the coupling between the slow and fast electron subsystems. The distribution function for the slow electrons is represented by: $f_s(t,\epsilon,\mathbf{\Omega})=f_0(t,\epsilon)+\mathbf{\Omega}\cdot\mathbf{f}_1(t,\epsilon)$, where $|\mathbf{f}_1|\ll|f_0|$ and $\mathbf{\Omega}$ is a unit vector in the direction of the electron's velocity. Assuming that the excitation and ionization cross sections are isotropic, Eq. (2) reduces to a pair of equations for f_0 and $\mathbf{f}_1$ (cf. [10]),

$$\frac{\partial f_0}{\partial t}-\frac{e}{3}\sqrt{\frac{2}{m\epsilon}}\frac{\partial}{\partial\epsilon}(\epsilon\mathbf{E}\cdot\mathbf{f}_1)=N\sqrt{\frac{2}{m\epsilon}}J_0^{st}[f_0]+S_{ion}^0,$$

$$\frac{\partial\mathbf{f}_1}{\partial t}-e\sqrt{\frac{2\epsilon}{m}}\mathbf{E}\frac{\partial f_0}{\partial\epsilon}-\frac{e\mathbf{B}_0}{mc}\times\mathbf{f}_1=-\sqrt{\frac{2\epsilon}{m}}NQ(\epsilon)\mathbf{f}_1(\epsilon), \tag{3}$$

where $Q=Q_{tr}+Q^*+Q^+$ is the total cross section of all collision processes and S_{ion}^0 is the source of slow electrons due to molecular ionization by the fast electrons, which will be discussed further in Sec. II C. The isotropic portion of the collision integral in Eq. (3) describes the energy exchange between the low energy electrons and molecules,

$$J_0^{st}[f_0]=\frac{2m}{M}\frac{\partial}{\partial\epsilon}[\epsilon^2 Q_{tr}(\epsilon)f_0]-\epsilon f_0(\epsilon)[Q^*(\epsilon)+Q^+(\epsilon)]$$
$$+\sum_k(\epsilon+\epsilon_k^*)Q_0^k(\epsilon+\epsilon_k^*)f_0(\epsilon+\epsilon_k^*)$$
$$+\int_{2\epsilon+\epsilon^+}^{\epsilon_g}dTTs^+(T,\epsilon)f_0(T)$$
$$+\int_{\epsilon+\epsilon^+}^{2\epsilon+\epsilon^+}dTTs^+(T,T-\epsilon-\epsilon^+)f_0(T), \quad (4)$$

where M is the mass of the molecules; ϵ_k^* and ϵ^+ are the molecular excitation thresholds for level k and for ionization, respectively; $s^+(\epsilon,T)$ is the ionization differential cross section; Q_{tr} is the transport cross section of elastic scattering; $Q^*=\Sigma_k Q_0^k$ is the total cross section of the excited molecules; and $Q^+=\int_0^{\epsilon_t}dTs^+(\epsilon,T)$, with $\epsilon_t=(\epsilon-\epsilon^+)/2$, is the cross section of the ionized molecules. Although Eq. (4) is written for a single species gas, its generalization to the multispecies case is straightforward.

B. Fast electron kinetics

In order to describe the kinetics of the fast electrons, the collision integral is first simplified and then approximated by assuming continuous deceleration and multiple pitch angle scattering [11]. Applying these approximations, the distribution function for the fast electrons, f_f, Eq. (2), according to [2,9,12], can be rewritten as

$$\frac{\partial f_f}{\partial t}-\frac{\partial}{\partial\epsilon}[(e\mathbf{\Omega}\cdot\mathbf{E}+F_D)vf_f]$$
$$-e\frac{\partial}{\partial\mathbf{\Omega}}\left\{\mathbf{\Omega}\times\left[\mathbf{E}\times\mathbf{\Omega}+\frac{v}{c}(\mathbf{B}+\mathbf{B}_0)\right]\frac{f_f}{p}\right\}=J_f^{st}+S_{ion}^f, \quad (5)$$

where F_D is the dynamic friction force that accounts for the energy losses of the fast electrons due to the continuous deceleration approximation [8] and is defined by the expression

$$F_D(\epsilon)=N\left[\frac{2m\epsilon}{M}Q_{tr}(\epsilon)+\sum_k\epsilon_k^*Q_0^k(\epsilon)+\epsilon^+Q^+(\epsilon)\right.$$
$$\left.+\int_0^{\epsilon_t}dTTs^+(\epsilon,T)\right]. \quad (6)$$

The three terms on the right-hand side of the equation describe the electron elastic scattering, molecular excitation, and molecular ionization, respectively, by the fast electrons. The source term, S_{ion}^f, on the right-hand side of Eq. (5) accounts for the production of fast electrons due to the ionization of neutral particles by fast particles. Finally, the term J_f^{st} is that part of the collision integral that accounts for the pitch angle scattering of the fast electrons: $J_f^{st}=vN\int d\mathbf{\Omega}'[f_f(\mathbf{\Omega}')-f_f(\mathbf{\Omega})]dQ(\mathbf{\Omega}\cdot\mathbf{\Omega}')$, where the differential cross section $dQ(\mathbf{\Omega}\cdot\mathbf{\Omega}')$ depends on the cosine of the scattering angle between the directions of incident, $\mathbf{\Omega}'$, and scattered, $\mathbf{\Omega}$, electrons. The left-hand side of Eq. (5) describes the orbits of the particles in terms of the change in the momentum of the electrons due to the Lorentz force and the dynamic frictional force, F_D. This part of the equation can be easily modeled by assuming macroparticles, because each of them follows a certain electron trajectory. A complications arises in the angular scattering term, J_f^{st}, on the right-hand side of Eq. (5), because it describes particles jumping from one orbit to another. This is a stochastic process, which can be modeled by using the Monte Carlo method [13]. However, applying the Monte Carlo method to simulate the scattering events in Eq. (5) requires a large number of particles to achieve an acceptably low level of fluctuations. This is especially inconvenient when solving the coupled equations (1) and (2), since the particle fluctuations generate additional fluctuations in the electromagnetic fields, which spread all over the whole volume of calculations with the speed of light. In order to avoid this problem, another deterministic approach was developed by using the orbital equations for the macroparticles and by accounting for multiple electron pitch angle scattering by following a simple semiempirical model proposed by Longmire [14]. In particular, it was suggested in Ref. [14] that another phase coordinate, in addition to the common phase coordinates ϵ and $\mathbf{\Omega}$, be introduced; that is, the average cosine of the scattering angle, $0<\mu<1$, of a macroparticle. This accounts for the effective deceleration of the macroparticles due to multiple scattering. In this case, the equations of motion of the macroparticles are

$$\frac{d\epsilon_q}{dt}=-ev_q\mathbf{\Omega}_q\cdot\mathbf{E}-v_qF_D(\epsilon_q), \quad \frac{d\mu_q}{dt}=-\mu_q v_q\Sigma_{tr},$$
$$\frac{d\mathbf{\Omega}_q}{dt}=-\frac{ev_q}{p_qc}\mathbf{\Omega}_q\times(\mathbf{B}+\mathbf{B}_0)-\frac{e}{p_q}\mathbf{\Omega}_q\times\mathbf{E}\times\mathbf{\Omega}_q, \quad (7)$$

where $\Sigma_{tr}=N\int d\mathbf{\Omega}'(1-\mathbf{\Omega}\cdot\mathbf{\Omega}')dQ(\mathbf{\Omega}'\cdot\mathbf{\Omega})=NQ_{tr}$ is the macroscopic transport cross section of electron scattering [8,9] and is defined as

$$\Sigma_{tr}=\frac{4\pi e^4NZ(Z+1)\gamma^2}{[mc^2(\gamma^2-1)]^2}\left(\ln\frac{1+\zeta}{\zeta}-\frac{1}{1+\zeta}\right) \quad (8)$$

and where Z is the atomic number on the gas atoms, $\gamma=1+\epsilon/mc^2$, and $\zeta=1.7\times10^{-5}Z^{2/3}(\gamma^2-1)^{-1}[1.13+3.76(Z/137)^2\gamma^2/(\gamma^2-1)]$. Each macroparticle q in Eq. (7) consists of an n_q electrons, which move approximately in the same direction, $\mathbf{\Omega}$, and the phase variable μ characterizes the average spread of electrons in the macroparticle in a perpendicular direction. Consequently, the distribution function of fast electrons is

$$f_f(t,\epsilon,\mathbf{\Omega},\mu)=\sum_q n_q\delta[\epsilon-\epsilon_q(t)]\delta[\mu-\mu_q(t)]$$
$$\times\delta[\mathbf{\Omega}-\mathbf{\Omega}_q(t)].$$

A newly formed particle normally does not have a spread, so that $\mu_q=1$. The pitch angle scattering increases the spread, which means that μ decreases with time according to the second equation (7). A macroparticle moves slower along its orbit as μ decreases, which must be taken into account when calculating the fast electron current: $\mathbf{j}_f=-e\Sigma_q n_q\mu_q\mathbf{v}_q$.

This model, Eq. (7), is convenient for performing numerical calculations; however, it possesses a significant drawback in that it is not conservative, since it incorrectly represents the energy balance in the system of particles and electromagnetic fields. To demonstrate this fact, the first equation of Eq. (7) is multiplied by n_q and summed over all macroparticles,

$$\sum_q n_q \frac{d\epsilon_q}{dt} = -e\mathbf{E}\sum_q n_q \mathbf{v}_q - \sum_q n_q \nu_q F_D . \tag{9}$$

The left-hand side of Eq. (9) represents the change in the overall electron kinetic energy per unit time. The second term on the right-hand side of this equation describes the energy losses due molecular excitation and ionization. The first term on the right-hand side should represent the work done by the electric field on the electrons and has the form $\mathbf{j}_f \cdot \mathbf{E}$. However, it is different by the factor μ_q in the expression for the electric current, which means that the electron energy is not conserved in Eq. (7).

Therefore, it is proposed to modify the Longmire model so that it would be conservative. This modified model can be derived from the kinetic equation, Eq. (5), by making some rather general assumptions. By multiplying Eq. (5) by ϵ and $\mathbf{\Omega}$ and integrating over a certain phase volume, one can derive equations for the average energy and velocity,

$$\begin{aligned} \frac{d}{dt}\langle \epsilon \rangle &= -\langle \nu F_D + e\nu \mathbf{\Omega}\cdot\mathbf{E}\rangle, \\ \frac{d}{dt}\langle \mathbf{\Omega}\rangle &= -e\left\langle \frac{\nu}{cp}\mathbf{\Omega}\times(\mathbf{B}+\mathbf{B}_0) + \frac{1}{p}\mathbf{\Omega}\times\mathbf{E}\times\mathbf{\Omega}\right\rangle + \Delta\mathbf{\Omega}^{st}. \end{aligned} \tag{10}$$

The angular brackets denote the average over the distribution function and $\Delta\mathbf{\Omega}^{st}$ is the average of the vector, $\mathbf{\Omega}$, with the pitch angle scattering term, J_f^{st}. The symmetry of the collision integral, $\int d\mathbf{\Omega} J_f^{st} = 0$, ensures that there is no contribution to the first equation of Eq. (10) and relates the last term of the second equation to the transport cross section (8). In fact, the quantity $\Delta\mathbf{\Omega}^{st}$ contains the following pitch angle integral:

$$\int d\mathbf{\Omega}\mathbf{\Omega}\int d\mathbf{\Omega}'[f_f(\mathbf{\Omega}') - f_f(\mathbf{\Omega})]dQ(\mathbf{\Omega}'\cdot\mathbf{\Omega}).$$

Changing the angular variables, $\mathbf{\Omega}' \to \mathbf{\Omega}$, in the first term of this expression and noting that the integral $\int d\mathbf{\Omega}'\mathbf{\Omega}' dQ$ is directed along the vector $\mathbf{\Omega}$, it can be shown that $\Delta\mathbf{\Omega}^{st} = -\langle \nu \mathbf{\Omega}\Sigma_{tr}\rangle$.

Although Eqs. (10) hold for average quantities, it is assumed that they are also valid for each macroparticle, since their motion is uncorrelated, the collisions between the fast electrons themselves are neglected and since only their collisions with the molecules are accounted for. However, there is a problem with the equation for $\langle\mathbf{\Omega}\rangle$ in Eq. (10). The unit length of this vector is not conserved because of the pitch angle scattering term. The decrease in $|\langle\mathbf{\Omega}\rangle|$ corresponds to the deceleration of the particles due to multiple scattering. This problem is resolved by following Longmire's idea and by attributing the change in the length of the vector $\mathbf{\Omega}_q$ of the macroparticle q to the effective pitch angle spread μ_q. Consequently, $\mathbf{\Omega}_q$ is redefined as $\mathbf{\Omega}_q \to \mu_q\mathbf{\Omega}_q$ and the new quantity, $\mathbf{\Omega}_q$, is required to be a unit vector. Thus, the second equation of Eqs. (10) separates into two equations and the macroparticle dynamics is governed by the following system of equations:

$$\begin{aligned} \frac{d\epsilon_q}{dt} &= -e\mu_q\nu_q\mathbf{\Omega}_q\cdot\mathbf{E} - \nu_q F_D(\epsilon_q), \\ \frac{d\mu_q}{dt} &= -\mu_q\nu_q\Sigma_{tr} - e\frac{1-\mu_q^2}{p_q}\mathbf{\Omega}_q\cdot\mathbf{E}, \\ \frac{d\mathbf{\Omega}_q}{dt} &= -\frac{e\nu_q}{cp_q}\mathbf{\Omega}_q\times(\mathbf{B}+\mathbf{B}_0) - \frac{e}{\mu_q p_q}\mathbf{\Omega}_q\times\mathbf{E}\times\mathbf{\Omega}_q . \end{aligned} \tag{11}$$

This set of equations constitutes the model that describes the dynamics of fast electrons. When compared to the original empirical model, Eq. (7), this new model is better justified by the fact that the average of the ensemble is a direct result of the kinetic equation (5). It can be seen that the change in the average pitch angle, μ_g, is also affected by the parallel component of the electric field.

To complete the description of fast electron kinetics, the source terms on the right-hand side of Eq. (5) must be specified. To do this, it is assumed that the secondary fast electrons produced by molecular ionization move mainly in a direction perpendicular to the momentum of the incident particles. Hence, the ionization source term, S_{ion}^f, is

$$\begin{aligned} S_{ion}^f = N\delta(\mathbf{\Omega})\delta(\mu-1)\int_{2\epsilon+\epsilon^+}^{\infty} d\epsilon' \int d\mathbf{\Omega}' \int_0^1 d\mu' \\ \times f_f(\epsilon',\mathbf{\Omega}',\mu')\nu' s^+(\epsilon',\epsilon), \end{aligned} \tag{12}$$

where $\epsilon > \epsilon_g$. The source term for the slow particles due to ionization by the fast electrons is

$$\begin{aligned} S_{ion}^0 = \frac{Nm^{3/2}}{4\pi\sqrt{2\epsilon}}\int_{2\epsilon+\epsilon^+}^{\infty} d\epsilon' \int d\mathbf{\Omega}' \int_0^1 d\mu' \\ \times f_f(\epsilon',\mathbf{\Omega}',\mu')\nu' s^+(\epsilon',\epsilon), \end{aligned} \tag{13}$$

where $\epsilon < \epsilon_g$. The newly liberated electrons are assumed to have an isotropic angular distribution.

C. Algorithm for numerical solution

In order to choose the proper numerical algorithm to solve the equations for the model, the dependence of the characteristics of the solution on electron energy must be taken into account. Since the fast electrons ($\epsilon > \epsilon_g$) are weakly collisional, a finite difference algorithm of second order accuracy can be used to calculate the trajectories of the fast electrons. To do this, a predictor-corrector iteration-free algorithm is used. At each time step, $\Delta t = t^{n+1} - t^n$, the trajectories of the fast particles are first integrated within the time interval $[t^n, t^{n+1}]$ using Eqs. (11). The ionization source terms, Eqs. (12) and (13), are then calculated and averaged over the time interval Δt. The decelerated particles are then identified and transformed into the corresponding sources of slow electrons in the Boltzmann equation. The Boltzmann equations for the slow electrons (3) are then integrated over Δt, taking into

account the production of new electrons by the ionization of molecules by the fast electrons according to Eq. (13). At the end of this step, the slow electrons have been accelerated to an energy of ϵ_g and are transformed into macroparticles. Then the time is advanced and Eqs. (11) integrated again, taking into account those new particles which were accelerated in the previous time step or which were generated due to ionization, Eq. (12). Since this proposed algorithm is not conservative, its accuracy was tested by checking the energy balance of the entire system.

The time step, Δt_g, used in the integration of the fast electron trajectories by using Eq. (11) can be chosen individually for each macroparticle within the full time step Δt, so that the relative variations in the macroparticle energy and the pitch angles are small: $\{\Delta\epsilon/\epsilon, \Delta\mu/\mu\} \ll 1$. If Δt_g is less than the main time step Δt when solving the Boltzmann equation, the equations for the macroparticle trajectories are integrated over the interval Δt several times.

The Boltzmann kinetic equations for slow electrons (3) have been solved by using a finite difference method of first order accuracy. The system of algebraic equations for discrete variables have been solved by using the Gauss exclusion method. Two complementary grids in the energy domain were introduced. The isotropic part of the electron distribution function was evaluated at K nodes, ϵ_i, where $i=1,\ldots,K$, while $\mathbf{f}_1$ was defined in the adjacent grid, $\epsilon_{i-1/2}=(\epsilon_i+\epsilon_{i-1})/2$, where $i=2,\ldots,K$ and $\epsilon_{1/2}=(3\epsilon_1-\epsilon_2)/2$. The last node of the second grid is the maximum energy of the slow electrons, $\epsilon_g=\epsilon_{K-1/2}$. All the slow electrons accelerated to this energy are transformed into fast electrons, thus reducing the slow electron population. Hence, the domain $\epsilon>\epsilon_g$ is an infinite sink of slow electrons and both functions f_0 and $\mathbf{f}_1$ have to equal zero at their last nodes: $f_0(\epsilon_K)=0$ and $\mathbf{f}_1(\epsilon_{K-1/2})=0$. These conditions have been tested at each time step after advancing the Boltzmann equations (3). If $f_0(\epsilon_K)$ and $\mathbf{f}_1(\epsilon_{K-1/2})$ are found not to be zero at the upper time limit, t^{n+1}, then a new macroparticle is injected and both functions are set equal to zero. The characteristics of this new macroparticle are defined by taking into account the conservation of the first moments of the electron distribution function, density, electric current, and average electron energy,

$$\mu_q=1, \quad \epsilon_q=\epsilon_K, \quad n_q=\delta n_s=2\pi(2/m)^{3/2}f_{0K}^{n+1}\sqrt{\epsilon_K}\Delta\epsilon_K,$$
$$en_q\mathbf{v}_q=-\delta j_s=e(2\pi/3)(2/m)^2\mathbf{f}_{1K-1/2}^{n+1}\epsilon_{K-1/2}\Delta\epsilon_{K-1/2}. \tag{14}$$

The reverse transformation of decelerated macroparticles into Boltzmann electrons is performed in a similar manner. If the particle energy, ϵ_q, at the upper time limit is found to be less than ϵ_g, then it is removed from the fast electron population and a corresponding number of slow electrons is generated. Two nodes, i and $i+1$, closest to the macroparticle energy ϵ_q^{n+1} were identified and the increments of the distribution functions, Δf_0 and $\Delta\mathbf{f}_1$, at these nodes and $\epsilon_{i+1/2}$ are calculated by using equations similar to Eqs. (14).

D. Code calibration

In order to test this model, the kinetics of secondary electrons produced by a single primary electron inserted at $t=0$ in an external dc electric field in molecular nitrogen was considered. The corresponding cross sections for the interaction of electrons with N_2 were obtained from [15–20]. The transport cross sections were taken from Ref. [15], and the fine structure of the resonant cross sections in the energy range from 1.8 to 4.0 eV was described according to [16]. The energy dependence of the first eight vibration excitation levels for N_2 were obtained from Ref. [17]; however, these cross sections were corrected according to the recommendations of [18]. The electron excitation cross sections were calculated by using the approximations proposed in Ref. [19], which are in good agreement with experimental data. The ionization cross sections of the first four electron energy levels were calculated by using the semiempirical formulas in [20].

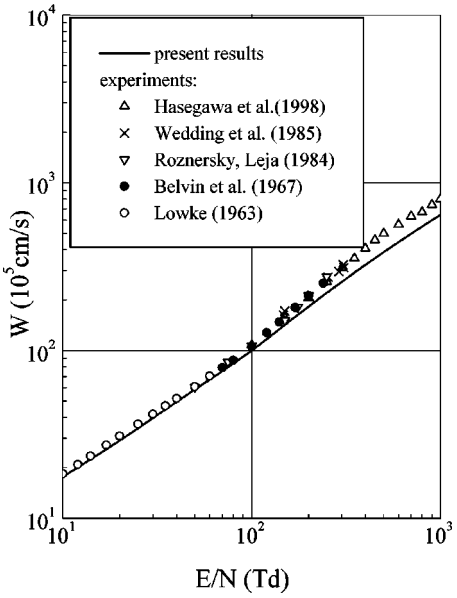

FIG. 1. Dependence of the electron drift velocity, W, in molecular nitrogen on the ratio of the applied electric field to the gas density, E/N. Solid line represents the simulation results. Points are the experimental data taken from Refs. [21–25].

The simulations were run until the asymptotic state was attained. This state is achieved when the secondary electrons drift in a direction opposite to the external electric field at a constant velocity of

$$W=-\frac{2\pi}{3n_e}\left(\frac{2}{m}\right)^2\int_0^{\epsilon_g}d\epsilon\,\epsilon\mathbf{e}\cdot\mathbf{f}_1(\epsilon,t), \tag{15}$$

where $\mathbf{e}$ is a unit vector in the direction of the dc electric field and $n_e(t)=2\pi(2/m)^{3/2}\int_0^{\epsilon_g}d\epsilon\sqrt{\epsilon}f_0(\epsilon,t)$ is the instantaneous density of free electrons. A comparison of the calculated electron drift velocity, W, with the experimental data tabulated in [21–25] is presented in Fig. 1. The older data from Refs. [24] and [25], which are complete and widely used in the literature [26], are in close agreement with recent measurements [27].

There is good agreement between the results of the simulations described in this paper and the available experimental data; however, there is a minor but systematic deviation for $E/N>100$ Td, where 1 Td equals 10^{-17} V cm^2. This underestimation of the drift velocity is due to the fact that all the

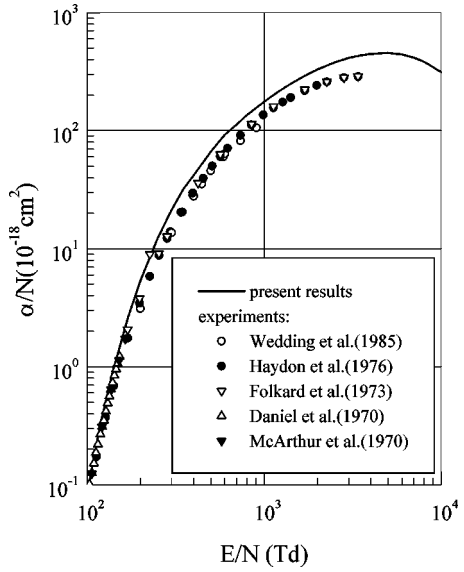

FIG. 2. Dependence of the electron ionization coefficient, α/N, in molecular nitrogen on the ratio of the applied electric field to the gas density, E/N. Solid line represents the simulation results. Points are the experimental data taken from Refs. [22,29–32].

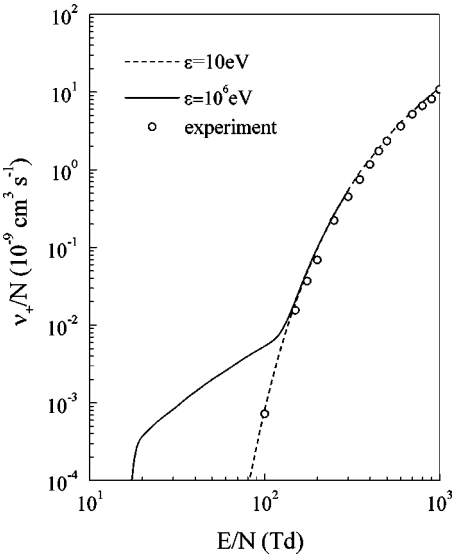

FIG. 3. Dependence of the electron ionization frequency, ν_+, in molecular nitrogen on the electric field, E/N. Lines represent the simulation results for the initial electron energy 1 MeV (solid line) and 10 eV (dashed line). Points are the experimental data.

cross sections were assumed to be isotropic. It has been demonstrated in Ref. [28] that for $E/N \sim 800$ Td, an approximation taking into account the anisotropy of the electron excitation cross sections leads to higher electron drift velocities, which turned out to be greater than the experimental data. Although the two-term kinetic model can take into account anisotropic cross sections, the experimental data are insufficient to verify the calculated results. Therefore, isotropic cross sections are used and the deviation shown in Fig. 1 demonstrates the accuracy of the model.

An additional illustration of the performance of the model is presented in Fig. 2, where the calculated electron ionization coefficient, $\alpha = \nu_+ / W$ is compared to the experimental electron swarm data published in [22,29–32]. In this case, the ionization frequency is defined as

$$\nu_+(t) \equiv \frac{1}{n_e}\frac{dn_e}{dt} = \frac{8\pi N}{m^2 n_e}\int_0^{\epsilon_g} d\epsilon \epsilon Q^+(\epsilon) f_0(\epsilon,t). \quad (16)$$

As can be seen in Fig. 2, the agreement between the simulations and the experimental data is excellent, with a minor deviation at very high electric fields; that is, $E/N \sim 1000$ Td. It should be noted that these high electric field values exceed the threshold values for the electron runaway effect. Although this effect has been accounted for in the model presented here and is discussed in the next section, it is unclear as to whether these runaway electrons have been detected under experimental conditions.

The above two examples demonstrate the accuracy of the model for the case of relatively slow electrons, but cannot be verified for fast electrons due to the unavailability of experimental data. The only well established fact is that the energy loss of a fast electron (with energy greater than 10 keV) in the production of single electron-ion pair, $\Delta\epsilon_{pair}$, does not depend on the electron energy and is equal to 36 eV for molecular nitrogen. When this case was simulated by using the model presented here, the calculated results were within 3% of the measured values. Apart from small discrepancies, the results shown in Figs. 1 and 2 demonstrate that the model presented in this paper accurately calculates the electron kinetics over a broad range of electron energies, electric fields, and gas pressures.

III. RUNAWAY EFFECTS IN THE GASES PREIONIZED BY GAMMA RAYS

A. Runaway electrons in dc discharge

The model described above has been used to study dc electric discharge in molecular nitrogen seeded with a relativistic electron. Possible sources of such electrons are cosmic rays or external gamma-ray sources. It is known that the drag force, F_D, has a minimum at an electron energy of $\epsilon_{crit} \sim 1.5$ MeV [1]. Therefore, if the applied electric field exceeds the critical field, $E_{crit} = F_D(\epsilon_{crit})/e$, the electrons with energy $\epsilon \lesssim \epsilon_{crit}$ might be accelerated and generate secondary high energy and low energy electrons through collisions with molecules. Avalanche gas breakdown caused by runaway electrons was first discussed qualitatively in [1]. However, quantitative analysis has been limited by the fact that in order to calculate the ionization rate more accurate electron-molecule collision cross sections must be used and the effects of multiple pitch angle scattering incorporated.

The critical electric field for the runaway effect to occur in molecular nitrogen is $E_{crit}/N \sim 10$ Td. Using the simulations presented in this paper, runaway avalanche breakdown was calculated to occur at electric fields $E/N > 14$ Td, provided that the initial energy of the electron, ϵ_0, falls within the runaway range; that is, $F_D(\epsilon_0) < eE$. The simulations were run until the ionization frequency and the electron drift velocity approached asymptotic values. The dependence of the ionization frequency (16) on electric field is presented in Fig. 3. The solid line represents the case where the initial energy of the seed electron is $\epsilon_0 = 1$ MeV (the high energy case), and the dashed line represents the reference case

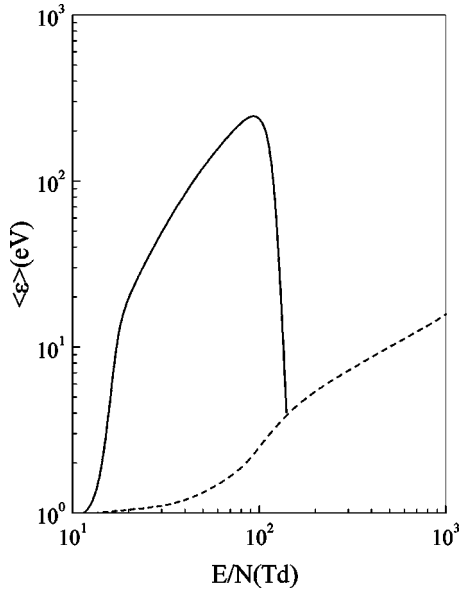

FIG. 4. Dependence of the average electron energy, $\langle\epsilon\rangle$, in molecular nitrogen on the electric field, E/N, for the initial electron energy 1 MeV (solid line) and 10 eV (dashed line).

where the initial energy of the seed electrons is $\epsilon_0 = 10\,\mathrm{eV}$ (the low energy case), which is well below the runaway threshold. It can be seen that the runaway electrons dominate the ionization process in the electric field range from 14 to 140 Td.

As can be seen in Fig. 3, the simulation results for the standard case (dashed line) are in good agreement with the experimental data represented by the open circles. The experimental data points were estimated in the following way: Using the electron drift velocities from [21] as a basis, the ionization coefficients measured by the New England group [29,30] was interpolated to the points where the drift velocities were measured. The final results, which are the product of W and α/N, are plotted in Fig. 3.

The runaway effect that occurs in electric discharge is also illustrated in Fig. 4, where the average electron energy,

$$\langle\epsilon\rangle = \frac{2\pi(2/m)^{3/2}\int_0^\infty d\epsilon\,\epsilon^{3/2} f_0(\epsilon) + \Sigma_q n_q \epsilon_q}{n_e + \Sigma_q n_q}, \qquad (17)$$

is plotted versus the effective electric field. The onset of discharge is manifested by the dramatic increase in electron energy. This occurs because of the presence of a small number of high energy electrons with energies ranging from tens of eV to a few MeV. These high energy electrons are completely responsible for the avalanche breakdown. The sharp increase in the average electron energy in the range from 14 to 140 Td is mainly due to the increase in the number of runaway electrons; however, their energy is also increased as the electric field increases. The average electron energy is more than three orders of magnitude less than the characteristic energy of fast electrons. If the slower electrons, with energies less than a few keV, are excluded from the integral in Eq. (17), the average energy of the fast electrons varies from 1 to 10 MeV in the electric field range from 14 to 140 Td. This difference in the average electron energy and the energy of the fast electrons is an indication that the majority

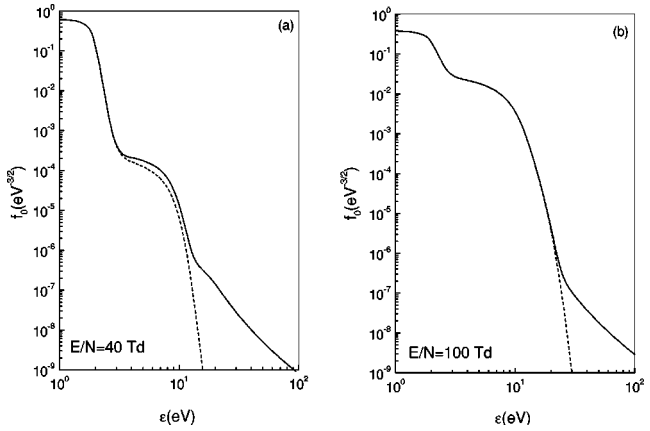

FIG. 5. Energy distribution of free electrons in the dc discharge in molecular nitrogen for the electric field $E/N = 40$ Td (a) and 100 Td (b). The initial electron energy $\epsilon_0 = 1$ MeV (solid line) and 10 eV (dashed line).

of the secondary free electrons, which are produced by a relativistic electron, have an energy of a few tens of eV. This fact can be observed in Fig. 5 in which the electron distribution functions are shown for both the fast and slow seed electrons. [The following normalization of the distribution function has been used in this figure: $2\pi(2/m)^{3/2}\int\sqrt{\epsilon} f_0(\epsilon)d\epsilon = 1$.] A significant difference arises between these two cases at electron energies in the range from 20 to 30 eV.

The average electron energy dependence on the electric field for the case of relativistic seed electrons differs dramatically from the case where the seed electron energy is low, since the average electron energy varies rather slowly as the electric field increases (dashed line in Fig. 4). Avalanche breakdown initiated by slow seed electrons begins at electric fields of about 140 Td, where the average electron energy exceeds the vibrational excitation states [33–35] of about 2 eV. It can be seen in Fig. 5, that the electron distribution function decreases three orders of magnitude at $\epsilon \approx 2$ eV for $E/N = 40$ Td, while at $E/N = 100$ Td, this decrease is less than one order of magnitude. The second drop in the electron distribution in Fig. 5 in the energy range of 10 eV is due to the electronic excitations of nitrogen molecules.

For larger electric fields, $E/N > 100$ Td, the dominant process is that by the slow electrons, since the relative number of slow electrons has increased significantly. This can be seen in Fig. 4 by the dramatic decrease in the average energy at $E/N \approx 100$ Td. Although the signatures of the fast electrons cannot be seen in the ionization frequency and in the average electron energy in Figs. 3 and 4, both the number and energy of the fast electrons increase. These fast electrons may be responsible for gamma-ray emissions from discharges and for other high energy phenomena.

B. Implications to the Ivy-Mike test

The Ivy-Mike test was conducted in 1952 and was one of the biggest thermonuclear ground tests in history [36]. One of the special features of this test is that multiple lightning discharges at distances from 900 to 1400 m from the center of the detonation were observed [4]. The strokes began near the ground and propagated upward along roughly concentric

paths around the burst throughout a time interval of 1–10 ms. The shape of the discharge paths, which were nearly circular with the burst point as the center, strongly suggests that they were driven by electric fields associated with electromagnetic pulses generated by the burst. Estimates indicate that the azimuthal electric files were 30 kV/m a few milliseconds after initiation of the detonation [5]. However, these estimates are two orders of magnitude lower than the dc electric field (3 MV/m) required to cause air to breakdown. There were investigations to understand the mechanism by which low amplitude breakdown occurs. It was suggested in Ref. [37] that ion clusters could be generated in the irradiated air due to ion–molecule reactions, which may significantly change the electrical characteristics of air. However, the experiments conducted at the Hermes-2 facility [38], where the absorbed radiation dose was ~ 10 Mrad, which is comparable to the Ivy-Mike test conditions, did not validate this hypothesis. Thus, the lightning discharges in the Ivy-Mike test have not been satisfactorily explained to date.

Recently, a new possible mechanism for initiating lightning discharges from a thunderstorm cloud to the ionosphere was proposed in [1]. This mechanism is based on the model for avalanche breakdown driven by runaway electrons accelerated by electric fields in the cloud. Electric fields having a magnitude an order of magnitude less than that of the dc fields can initiate the runaway avalanche breakdown. It was thought in Refs. [1,2] that the seed electrons required to initiate this process were produced by cosmic rays. A similar process can be used to explain the discharges observed in the Ivy-Mike test, with the exception that the seed electrons are Compton electrons. The test conditions were favorable for initiating avalanche breakdown by runaway electrons. Exceptionally high neutron yield by the thermonuclear reaction and secondary gamma-ray emission were the sources of a large number of free electrons with characteristic energies ranging up to 1 MeV in air. These electrons might runaway in the electric fields near the tips of antennas and initiate air breakdown.

Unfortunately, there is no comprehensive theory for electric discharges in air from elongated metal structures like antennas and lightning rods. However, an empirical criteria for air breakdown, $E_0 h > 1$ MV, has been derived [39], where h is the height of the antenna and E_0 is the electric field near the surface of the earth. This criterion is valid for ground-to-cloud lightning discharges under normal, nonnuclear conditions, but would be relaxed if runaway electrons are present. Using the model proposed in this paper, simulations show that seed electrons with an initial energy of 1 MeV produce secondary runaway electrons and initiate avalanche breakdown in electric fields with magnitudes more than 5 times less than at normal atmospheric conditions. Although these simulations assume spatially homogeneous dc electric fields, it is speculated that similar results will be obtained in the inhomogeneous fields of antennas. Therefore, it is suggested that the criterion for achieving air breakdown in the Ivy-Mike test is that the electric fields must be greater than $E_0 h \sim 0.2$ MV. For antennas with a height of 10 m, the breakdown electric field is estimated to be 20 kV/m, which is less than the fields estimated for the Ivy-Mike EMP environment. More detailed studies of the effects of radiation-induced runaway electrons on electric breakdown will be presented in future papers.

IV. CONCLUSIONS

In conclusion, a model was developed to simulate the kinetics of electrons driven by electromagnetic pulses propagating through the atmosphere. This model takes into account the molecular excitation and ionization processes due to electron collisions. An important characteristic of this model is that it also takes into account fast electrons, which may be accelerated in quasistatic electric fields and run away. These fast electrons are treated as a separate system of macroparticles that can pass back and forth between the ensemble of fast and slow electrons. The algorithms used to perform the numerical calculations were briefly discussed and the numerical code was tested for the case of avalanche breakdown in air in an external dc electric field. The parameters used in the numerical calculations were chose to ensure necessary accuracy and good performance of the code.

The proposed electron kinetic model constitutes the main enhancement to existing hydrodynamic codes. This new code can be applied to the study of the various effects associated with the propagation and interaction of intense electromagnetic pulses in air and the effects of runaway electrons. Using this model, estimates and simulations suggest that the runaway effect of radiation-induced electrons may explain the multiple lightning discharges observed in the Ivy-Mike thermonuclear test.

ACKNOWLEDGMENTS

The authors are grateful to R. A. Roussel-Dupré, E. M. D. Symbalisty, and V. A. Yukhimuk of Los Alamos National Laboratory, and A. V. Gurevich and K. P. Zybin of P. N. Lebedev Physics Institute for a number of useful discussions and comments. This work was supported by the International Science and Technology Center under Project No. 311-96 and, in part, by the Russian Foundation for Basic Research under Grant No. 99-02-17267.

[1] A. V. Gurevich, G. M. Milikh, and R. A. Roussel-Dupré, Phys. Lett. A **165**, 463 (1992).

[2] R. A. Roussel-Dupré, A. V. Gurevich, T. Tunnell, and G. M. Milikh, Phys. Rev. E **49**, 2257 (1994); E. M. D. Symbalisty, R. A. Roussel-Dupré, and V. A. Yukhimuk, IEEE Trans. Plasma Sci. **26**, 1575 (1998).

[3] S. V. Bulanov, M. Lontano, and P. V. Sasorov, Phys. Plasmas **4**, 931 (1997).

[4] M. A. Uman, D. F. Seacord, G. H. Price, E. T. Pierce, J. Geophys. Res. **77**, 1591 (1972).

[5] R. D. Hill, J. Geophys. Res. **78**, 6355 (1973); M. K. Grover, IEEE Trans. Nucl. Sci. **NS-28**, 990 (1981); R. L. Gardner

et al., Phys. Fluids **27**, 2694 (1984); J. D. Colvin *et al.*, J. Geophys. Res. **92**, 5696 (1987); E. R. Williams *et al.*, J. Geophys. Res. **93**, 1679 (1988).

[6] P. Shkarofsky, T. W. Johnston, and M. P. Bachynski, *The Particle Kinetics of Plasmas* (Addison-Wesley, Reading, MA, 1966).

[7] A. I. Golubev, M. D. Kamchibekov, A. V. Soldatov, T. G. Sysoeva, V. A. Terekhin, and V. T. Tikhonchuk, *Electromagnetic Waves and Electronic Systems* (Publishing House of the Journal Radiotekhnika, Moscow, 1998), Vol. 3, pp. 93–99.

[8] H. A. Bethe, Ann. Phys. (N.Y.) **5**, 325 (1930).

[9] C. D. Zerby and F. L. Keller, Nucl. Sci. Eng. **27**, 190 (1967).

[10] Yu. A. Taranenko, U. S. Inan, and T. F. Bell, Geophys. Res. Lett. **20**, 1539 (1993).

[11] S. A. Goudsmit and J. L. Saunderson, Phys. Rev. **57**, 24 (1940); **58**, 36 (1940).

[12] A. V. Gurevich, R. Roussel-Dupré, and K. P. Zybin, Phys. Lett. A **237**, 240 (1998); **243**, 362 (1998).

[13] N. V. Ivanov and Yu. K. Kochubei, Vopr. At. Nauki Tech., Ser.: Metodiki Programmy, **1**(9), 18 (1982).

[14] C. L. Longmire, IEEE Trans. Nucl. Sci. **NS-22**, 2340 (1975); C. L. Longmire, IEEE Trans. Antennas Propag. **AP-26**, 3 (1978); W. R. Zimmerman, C. L. Longmire, IEEE Trans. Nucl. Sci. **NS-34**, 651 (1978).

[15] M. Hayashi, Institute Plasma Phys., Nagoya University, Japan, Report No. IPPJ-AM-19, 1981.

[16] W. Sun, M. A. Morrison, W. A. Isaacs, W. K. Trail, D. T. Alle, R. J. Gulley, M. J. Brennan, and S. J. Buckman, Phys. Rev. A **52**, 1229 (1995).

[17] G. J. Schulz, Phys. Rev. **135**, 988 (1964).

[18] I. Shimamura, Sci. Paper Inst. Phys. Chem. Res., Japan **82**, 1 (1989).

[19] T. Murphy, Los Alamos National Laboratory, Report No. LA 11288-MS, 1988.

[20] Y.-K. Kim, M. E. Rudd, Phys. Rev. A **50**, 3954 (1994); Hwang, Y.-K. Kim, M. E. Rudd, J. Chem. Phys. **104**, 2956 (1996).

[21] H. Hasegawa *et al.*, J. Phys. D **31**, 737 (1998).

[22] A. B. Wedding *et al.*, J. Phys. D **18**, 2361 (1985).

[23] W. Roznerski and K. Leja, J. Phys. D **17**, 249 (1984).

[24] H. A. Belwin *et al.*, Aust. J. Phys. **20**, 741 (1967).

[25] J. J. Lowke, Aust. J. Phys. **16**, 115 (1963).

[26] L. G. H. Huxley and R. W. Crompton, *The Diffusion and Drift of Electrons in Gases* (Wiley, New York, 1974).

[27] Y. Nakamura *et al.*, J. Phys. D **20**, 933 (1987).

[28] S. A. J. Al-Amin *et al.*, J. Phys. D **18**, 2007 (1985).

[29] S. C. Haydon *et al.*, J. Phys. D **9**, 523 (1976).

[30] M. A. Folkland and S. C. Haydon, J. Phys. B **6**, 214 (1973).

[31] McArthur *et al.*, Proceedings of the First International Conference on Gas Discharges, London (Institution of Electrical Engineers, London, 1970), p. 284.

[32] Daniel *et al.*, J. Phys. B **3**, 363 (1970).

[33] In molecular nitrogen the friction force demonstrates a pronounced maximum in the range 2–4 eV due to the excitation of vibrational levels [34,35]. It prevents the electron acceleration in weak electric fields above the energy of 2 eV.

[34] S. P. Sinker, A. W. Ali, and R. D. Taylor, J. Appl. Phys. **67**, 679 (1990).

[35] T. Majeed and D. J. Strickland, J. Phys. Chem. Ref. Data **25**, 335 (1997).

[36] F. H. Shelton, *Reflections of a Nuclear Weaponeer* (Shelton Enterprise, Colorado Springs, 1988).

[37] M. Scheibe (unpublished).

[38] J. G. Chervenak and V. A. J. Van Lint, IEEE Trans. Nucl. Sci. **NS-27**, 1810 (1980); **NS-29**, 1880 (1982).

[39] E. T. Pierce (unpublished).